

See discussions, stats, and author profiles for this publication at: <https://www.researchgate.net/publication/326467023>

Benchmarking of an additive manufacturing process

Conference Paper · July 2018

CITATIONS

0

READS

264

7 authors, including:



Vicente M Rivas Santos

University of Nottingham

2 PUBLICATIONS 0 CITATIONS

[SEE PROFILE](#)



Ian Maskery

University of Nottingham

54 PUBLICATIONS 658 CITATIONS

[SEE PROFILE](#)



Danny Sims-Waterhouse

University of Nottingham

14 PUBLICATIONS 29 CITATIONS

[SEE PROFILE](#)



Adam Thompson

University of Nottingham

33 PUBLICATIONS 132 CITATIONS

[SEE PROFILE](#)

Some of the authors of this publication are also working on these related projects:



Design for Metrology in Additive Manufacturing [View project](#)



Reference algorithms and metrology on aspherical and freeform optical lenses (FreeFORM) [View project](#)

BENCHMARKING OF AN ADDITIVE MANUFACTURING PROCESS

Vicente M. Rivas Santos¹, Ian Maskery², Danny Sims-Waterhouse¹, Adam Thompson¹, Richard Leach¹, Adam Ellis³ and Peter Woolliams⁴

¹Manufacturing Metrology Team, Faculty of Engineering, University of Nottingham, UK

²Centre for Additive Manufacturing, Faculty of Engineering, University of Nottingham, UK

³Xaar plc, Nottingham, UK

⁴National Physical Laboratory, Teddington, UK

INTRODUCTION

To accurately assess the performance of an additive manufacturing (AM) system, an analysis of its building capabilities is needed. In this paper, a benchmarking artefact for AM quality testing is measured following established methods. The use of benchmarking artefacts to test AM systems has been the subject of previous work [1], but these studies usually lack a deep metrological analysis. The measurements that we provide are obtained with three different systems: a contact coordinate measuring machine (CMM), a non-contact photogrammetry system (PG) and an X-ray computed tomography system (XCT). The benchmarking artefact (figure 1) was designed for a powder bed fusion AM process [2]; in particular, high-speed sintering (HSS) [3]. HSS is a powder bed fusion process in which a polymer is sintered by an infrared lamp with the aid of an infrared-absorbing jetted ink. The HSS process provides freedom of design and does not need supports structures. The measurement results of the benchmarking

artefact provide information about the performance of the AM system through the analysis of basic benchmarking features: sphericity, cylindricity, parallelism, coaxiality, minimum feature dimensions and build angles.

Design-for-metrology is a methodology in development at the University of Nottingham, aiming to improve and facilitate measurements of AM parts. Design-for-metrology ensures that the characteristics, limitations and standard procedures of available measurement systems are taken into account at the component design stage [2]. The necessity for this methodology comes from the increased complexity of AM parts compared with traditionally manufactured parts. AM parts often include internal features, lattice structures, cavities and freeform geometries which present serious challenges for current metrology systems [4]. Complementing this methodology development, new metrology systems are being developed at the University of Nottingham to overcome these challenges [5].

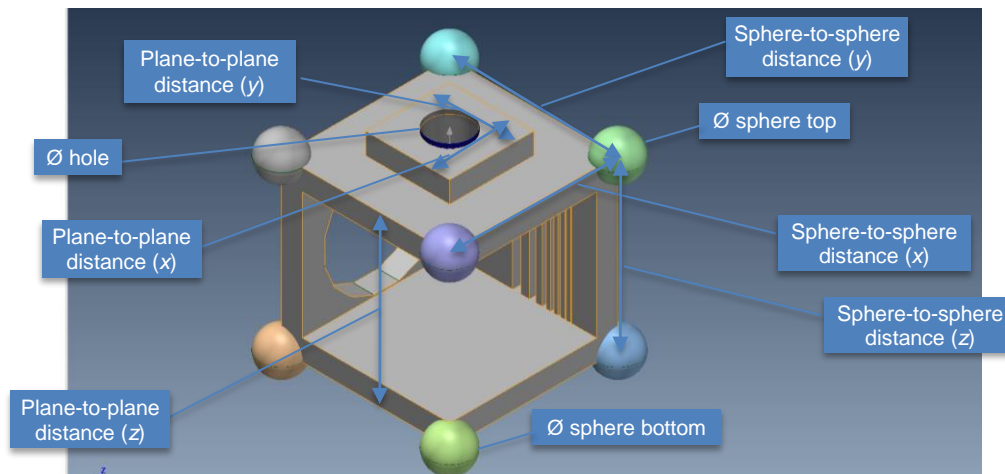


FIGURE 1. CAD model of the artefact with some of the features analysed in this paper highlighted.

A benchmarking artefact was previously designed for use with an HSS system. The artefact was created to test the system performance due to the absence of an industrial standard benchmark for AM machines. The artefact consists of a hollow cube with a side length of 40 mm, featuring spheres of 5 mm radius at each vertex. Each face of the cube possesses a range of features to provide information about the AM system: parallel planes, holes, cylinders, features of decreasing dimension, inclined planes and spheres.

MEASUREMENTS

Contact CMM

A traceable CMM at the National Physical Laboratory (NPL) was used to measure the artefact. The reliability and standardisation of CMMs make them ideally suited to provide a traceable dataset for comparison with other measurement systems. CMMs tend to be slower than other methods, as well as register a low number of points. Measurement time is another factor to consider, with high detailed planning of the measurement being necessary as well as the slow point acquisition.

The CMM used was a Mitutoyo Crysta S Apex 776, with a 55 mm long, 1 mm diameter ball-tipped stylus, and a probing deflection of 0.2 mm. Measurements were made in a temperature-controlled laboratory at $(20 \pm 2)^\circ\text{C}$. The CMM had a maximum permissible measuring error $E_0 = 1.7 + 3L \mu\text{m}$ (where L is the test length in millimetres) and a maximum permissible probing error $P_{FTU} = 1.7 \mu\text{m}$ [6]. The uncertainty simulations of the CMM measurements were carried out using PUNDIT CMM5 software [7]. For the uncertainty simulations, the following parameters were added to the model: a measured temperature of $(20 \pm 1)^\circ\text{C}$, a linear coefficient of thermal expansion (assumed) $\alpha = (8 \pm 1) \times 10^{-5} \text{ K}^{-1}$ and a mean roughness depth, R_z of 25 μm , 50 μm and 75 μm . More than one value of R_z was tested to better understand the importance of roughness on the uncertainty calculation. The roughness R_z was measured at Nottingham with a contact stylus instrument, with a value of $(50 \pm 3) \mu\text{m}$. The CMM measurements with uncertainty statements help to assess the reliability of the measurements against the resolution of the AM system.

Photogrammetry

Photogrammetry is a measurement technology based on the triangulation of points from many images. The expanded uncertainties [8] of 20 μm that photogrammetry can achieve is generally larger than CMMs (usually with maximum permissible errors lower than 10 μm), but photogrammetry can provide high density point clouds for complex AM parts at relatively high speeds. Additionally, the observable texture on samples produced by the HSS system produces strong correspondence between images, allowing high-density point clouds to be produced. Despite time-consuming reconstruction algorithms, high-speed data acquisition makes the measurement process faster and cheaper than the other two methods provided here (CMM and XCT). Photogrammetry measurements were made in a temperature-controlled laboratory at $(20 \pm 0.5)^\circ\text{C}$ at the University of Nottingham. The scaling factor for the point cloud was obtained using the distance between centres of spheres obtained with the CMM, due to its low uncertainty, 0.006 μm . The uncertainty of the scaled reconstruction was then evaluated using a combination of the CMM uncertainty and sphere to sphere uncertainties evaluated in previous work [8].

X-ray computed tomography

X-ray computed tomography (XCT) is a measurement technique that uses X-rays to produce volumetric representations of an object [9]. The main advantage of XCT compared to other measurement techniques is its ability to detect the internal features of a component non-destructively. Although typically more expensive than the other options presented, XCT is the only way to obtain measurements for the most complex AM geometries. XCT is also typically more time-consuming than other non-contact measurement methods due to the high number of projections needed for the measurements. XCT is also able to provide internal defect and porosity information of AM parts. The XCT system used here was a Nikon MCT 225, with a quoted maximum permissible error, $MPE = 9 + L/50 \mu\text{m}$ (where L is the test length in millimetres) and a temperature-controlled cabinet at $(20 \pm 0.1)^\circ\text{C}$, which is itself in a temperature-controlled laboratory at $(20 \pm 0.5)^\circ\text{C}$. Due to the high complexity of the XCT system, measurements are provided with an uncertainty analysis comprising an addition in quadrature of the MPE and the statistical experimental uncertainty.

The following parameters were used for XCT measurement: voltage 110 kV, current 318 μ A, 3142 projections, exposure 2 s and gain 24 dB. A detector shading correction was applied by averaging 256 reference frames (128 bright and 128 dark) and a warmup scan of approximately one hour was performed prior to a batch of three repeated scans. A 0.75 mm copper pre-filter was used between the X-ray source and the artefact. X-ray imaging and volumetric reconstruction were performed using the manufacturer's proprietary software (X-Inspect and CT-Pro, respectively), using the FDK algorithm [10] with a first order beam hardening correction and a Ramp noise filter, with cut-off at the maximum spatial frequency. Following reconstruction, XCT data were imported into Volume Graphics VGStudioMAX 3.0 [11] and surfaces were determined using the local maximum gradient algorithm over a search distance of four voxels, beginning from the ISO 50 % isosurface [12].

RESULTS AND DISCUSSION

Calculations of the uncertainty of the CMM measurements were made for different roughness values (see Table 1, where the uncertainty values of the sphere diameters are shown). The uncertainty calculations of the CMM measurements showed a high dependence of the surface roughness characteristic of AM parts. Previous research shows values of R_z between 30.78 μ m and 74.99 μ m for a selectively laser sintered polyamide [13], so 25 μ m, 50 μ m and 75 μ m values of R_z were used for the uncertainty calculations, with the aim of having a better indication of the CMM measurements uncertainty of the of the process under different printing parameters.

TABLE 1. Uncertainty values for a 10 mm diameter sphere obtained for the CMM measurements with variations on the R_z

R_z (mm)	Uncertainty of a 10 mm \varnothing sphere (mm)
0.025	0.03
0.050	0.05
0.075	0.08

The measurements of the external diameters are larger on the CMM than the XCT and the photogrammetry systems, while the internal diameters are measured smaller (see Table 2). All these measurements had a nominal value on the CAD model of 10 mm. The measurements follow the systematic difference between XCT and contact CMM shown elsewhere [14], where the measured external diameter of a cylinder on an XCT system is smaller than the CMM measurement by approximately $R_z/2$, while internal diameters are larger than CMM values by $R_z/2$.

TABLE 2. Measurements for the sphere, cylinder and hole diameter features.

Feature	XCT (mm)	CMM (mm)	PG (mm)
\varnothing sphere top	9.896 \pm 0.019	10.22 \pm 0.05	10.05 \pm 0.04
\varnothing sphere bottom	9.911 \pm 0.019	10.28 \pm 0.05	9.98 \pm 0.04
\varnothing hole	10.04 \pm 0.02	9.99 \pm 0.05	10.09 \pm 0.04
\varnothing cylinder	9.94 \pm 0.02	9.94 \pm 0.05	9.94 \pm 0.04

The linear distance between spheres centres (see table 3) allows a better understanding of the dimensional precision of the AM system, due to their low uncertainties and better measurement precision. The system shows a slight shrinkage in the horizontal plane (the CAD model has a 40 mm distance between spheres centres) and an expansion along the z axis. The shrinkage in the horizontal plane is not affected by the direction, so its cause is not directly related to the inkjetting process or the machine movement. The plane-to-plane distances show a larger difference compared to the CAD values than the sphere-to-sphere distance. This originates from the high surface roughness resulting from the HSS process. In the plane-to-plane distance, the photogrammetry results show a higher value than the other two measurement methods, and its precision decays greatly with the increase of the distance measured.

TABLE 3. Results for the plane-to-plane and sphere-to-sphere distance of the different measurement instruments.

Feature	XCT (mm)	CMM (mm)	PG (mm)
Plane-to-plane distance (x)	19.89 ± 0.02	19.88 ± 0.06	19.93 ± 0.04
Plane-to-plane distance (y)	19.923 ± 0.019	19.93 ± 0.05	19.99 ± 0.04
Plane-to-plane distance (z)	39.86 ± 0.02	39.98 ± 0.05	40.02 ± 0.04
Sphere-to-sphere distance (x)	39.943 ± 0.019	39.947 ± 0.006	39.95 ± 0.04
Sphere-to-sphere distance (y)	39.929 ± 0.019	39.947 ± 0.006	39.96 ± 0.04
Sphere-to-sphere distance (z)	40.09 ± 0.02	40.109 ± 0.006	40.13 ± 0.04

CONCLUSIONS

The results provide information about the performance of the HSS system, helping to establish operating parameters for the process. They also demonstrate the effectiveness of the benchmarking artefact design. The spheres that the artefact provide allow for effective comparison between different measurements systems. The results show the high dependence on surface roughness on the uncertainty values for the CMM. These uncertainty values are relatively large in comparison with other traditional manufacturing processes such as machining. Those high uncertainties can difficult the use of AM parts for precision applications. To overcome this obstacle, improvements either on the measurements or on the printing processes are needed, Uncertainty values are lower on the non-contact systems for the measurement of features other than the sphere-to-sphere distances, but standardisation has not been provided, so their use on industrial applications should be used with caution. The results show that CMM may not be the most effective system for the reference measurement of AM parts, and non-contact systems maybe be more adequate.

REFERENCES

- [1] Rebaioli L, Fassi I. A review on benchmark artifacts for evaluating the geometrical performance of additive manufacturing processes. *International Journal of Advanced Manufacturing Technology*. 2017; 93: 2571–2598.
- [2] Rivas Santos VM, Sims-waterhouse D, Piano S, et al. Metrological design of calibration and benchmarking artefacts for an additive manufacturing system. *Dimensional Accuracy and Surface Finish in Additive Manufacturing*. Leuven, 2017; 24–27.
- [3] Ellis A, Noble CJ, Hopkinson N. High Speed Sintering: Assessing the influence of print density on microstructure and mechanical properties of nylon parts. *Additive Manufacturing*. 2014; 1–4: 48–51.
- [4] Thompson MK, Moroni G, Vaneker T, et al. Design for Additive Manufacturing: Trends, opportunities, considerations, and constraints. *CIRP Annals - Manufacturing Technology* 2016; 65: 737–760.
- [5] Stavroulakis PI, Chen S, Sims-Waterhouse D, et al. Combined use of a priori data for fast system self-calibration of a non-rigid multi-camera fringe projection system. *Modeling Aspects in Optical Metrology VI*. Munich, 2017; 1033006.
- [6] ISO. 10360 Geometrical product specifications (GPS) Acceptance and reverification tests for coordinate measuring machines (CMM). 2009.
- [7] Beaman J, Morse E. Experimental evaluation of software estimates of task specific measurement uncertainty for CMMs. *Precision Engineering*. 2010; 34: 28-33.
- [8] Sims-Waterhouse D, Piano S, Leach R. Verification of micro-scale photogrammetry for smooth three-dimensional object measurement. *Measurement Science and Technology*. 2017; 28: 55010–16.
- [9] Thompson A, Maskery I, Leach RK. X-ray computed tomography for additive manufacturing: a review. *Measurement Science and Technology*. 2016; 27: 72001–18.
- [10] Hermanek P, Sing J, Rathore, et al. Principles of X-ray Computed Tomography. *Industrial X-ray computed*

- tomography. Springer, New York: 2017; 25–68.
- [11] Volume Graphics. VGStudio MAX.
 - [12] Kiekens K, Welkenhuyzen F, Tan Y, et al. A test object with parallel grooves for calibration and accuracy assessment of industrial computed tomography (CT) metrology. *Measurement Science and Technology*. 2011; 22: 115502.
 - [13] Sachdeva A, Singh S, Sharma VS. Investigating surface roughness of parts produced by SLS process. *International Journal of Advanced Manufacturing Technology*. 2013; 64: 1505–1516.
 - [14] Aloisi V, Carmignato S. Effect of surface roughness on uncertainty of X-ray CT dimensional measurements of additive manufactured parts. *Case Studies in Nondestructive Testing and Evaluation*. 2015; 6: 104–106.